(NASA-TM-78164) SIMPLIFIED MODEL OF STATISTICALLY STATIONARY SPACECRAFT ROTATION AND ASSOCIATED INDUC'D GRAVITY ENVIRONMENTS (NASA) 43 p HC A03/MF A01 CSCL 22B

N78-21198

Unclas
G3/18 11920

NASA TECHNICAL MEMORANDUM

NASA TM - 78164

SIMPLIFIED MODEL OF STATISTICALLY STATIONARY SPACECRAFT ROTATION AND ASSOCIATED INDUCED GRAVITY ENVIRONMENTS

By George H. Fichtl and Robert L. Holland
Space Sciences Laboratory

February 1978

NASA

George C. Marshall Space Flight Center
Marshall Space Flight Center, Alabama

1. Report No.
NASA TM-78164

2. Government Accession No.

3. Recipient's Catalog No.

4. Title and Subtitle

Simplified Model of Statistically Stationary Spacecraft Rotation and Associated Induced Gravity Environments

5. Report Date
February 1978

6. Performing Organization Code

7. Author(s)
George H. Fichtl and Robert L. Holland

8. Performing Organization Report No.

9. Performing Organization Name and Address
George C. Marshall Space Flight Center
Marshall Space Flight Center, Alabama 35812

10. Work Unit No.

11. Contract or Grant No.

13. Type of Report and Period Covered
Technical Memorandum

12. Sponsoring Agency Name and Address
National Aeronautics and Space Administration
Washington, D.C. 20546

14. Sponsoring Agency Code

15. Supplementary Notes
Prepared by Space Sciences Laboratory, Science and Engineering.

16. Abstract

A simplified stochastic model of spacecraft motion is developed. The model is based on the assumption that the net torque vector due to crew activity and rocket thruster firings is a statistically stationary Gaussian vector process. The process has zero ensemble mean value, and the components of the torque vector are mutually stochastically independent. Each component of the torque vector is characterized by a constant, nonzero, spectral density function in the frequency interval $\omega_1 < |\omega| \le \omega_0$ with zero spectral density for all other values of ω. The linearized rigid-body equations of motion are used to derive the autospectral density functions of the components of the spacecraft rotation vector which are shown to be proportional to ω^{-2} over the interval $\omega_1 < |\omega| \le \omega_0$ and zero for all other values of ω. The cross-spectral density functions of the components of the rotation vector vanish for all frequencies so that the components of rotation are mutually stochastically independent. The autospectral and cross-spectral density functions of the induced gravity environment imparted to scientific apparatus rigidly attached to the spacecraft are calculated from the rotation rate spectral density functions via linearized inertial frame to body-fixed principal axis frame transformation formulae. The autospectral and cross-spectral densities of the induced gravity vector components are equal to nonzero constants over the frequency interval $\omega_1 < |\omega| \le \omega_0$; however, the cross-spectral density functions are less than zero, thus indicating negative correlation between any two unlike induced gravity components in the principal axis frame of the vehicle. The induced gravity process is a Gaussian one with zero mean value. Transformation formulae are used to rotate the principal axis body-fixed frame to which the rotation rate and induced gravity vectors are referred to a body-fixed frame in which the components of the induced gravity vector are stochastically independent.

Rice's theory of exceedances is used to calculate expected exceedance rates of the components of the rotation and induced gravity vector processes. Application of the assumption that the number of exceedances of rotation rate and induced gravity over a given duration time T are Poisson distributed permits calculation of the risks associated with the components of the rotation rate and induced gravity vectors exceeding specified critical values at least once as a function of experiment duration time.

17. Key Words (Suggested by Author(s))

18. Distribution Statement
George H. Fichtl
Unclassified — Unlimited

19. Security Classif. (of this report)	20. Security Classif. (of this page)	21. No. of Pages	22. Price
Unclassified	Unclassified	43	NTIS

TABLE OF CONTENTS

LIST OF ILLUSTRATIONS

LIST OF ILLUSTRATIONS (Concluded)

TECHNIC ʟL MEMORANDUM 78164

SIMPLIFIED MODEL OF STATISTICALLY STATIONARY SPACECRAFT ROTATION AND ASSOCIATED INDUCED GRAVITY ENVIRONMENTS

I. INTRODUCTION

Space vehicle rotations resulting from crew activity, thruster firings, etc., and the associated induced g environments appear to be stochastic in character. Accordingly, to define an experiment to be performed aboard a space vehicle which is sensitive to vehicle rotations and the associated induced g environments, it would appear that statistical information concerning the risk of exceedance of critical rotation rates and g levels would be extremely useful. Clearly, the statistics of space vehicle motions and associated induced g environments depend on the vehicle mass and geometry properties, the dynamic behavior of the crew (push-off, sneezing, etc.), the control system parameters, the mission profile, etc. Estimates of these statistics can be obtained from Monte Carlo simulation of the vehicle/forcing function system or from postflight analysis of g environment time histories acquired from onboard instrumentation (accelerometers, rate gyros) or look angle data. However, estimates of statistics of space vehicle motions and the associated induced g levels do not appear to be available at this time for the currently planned Space Transportation System (STS) missions with payloads involving g sensitive experiments (for example, those on Spacelab missions 1 and 3) other than estimates of typical and worst case rotations and associated g levels resulting from various kinds of discrete vehicle excitations.[1] Furthermore, statistical summaries of vehicle rotation and associated g environments measured on previous space flight missions do not appear available. However, a number of excellent reports are available on the effects of crew motion on spacecraft attitude. Reference 1 documents the results of detailed simulations of the effects of crew motion on Apollo vehicle attitude, and Reference 2 provides the results of crew motion experiments conducted during the Skylab Program. This report attempts to provide estimates of exceedance statistics of vehicle rotations and associated g environments resulting from space vehicle motions.

1. Lewis, R., Private Communication, 1978.

The approach taken involves the use of basic assumptions concerning the statistics of the torque imposed on a spacecraft resulting from crew activity and thruster firings, i.e., that the imposed components of torque constitute a Gaussian process wherein the associated spectrum of torque in the frequency domain is that associated with a band-limited noise process with constant, nonzero spectral density over the frequency bandwidth of the process and zero spectral density for frequencies outside the bandwidth. The rigid-body equations of motion are used to derive the statistics of the spacecraft rotations. Finally, the statistics of the associated g environments are derived from the vehicle rotation statistics by applying transformation formulae between inertial and rotating frames. The mathematical machinery of Rice's theory of exceedances is used to obtain estimates of expected temporal rates of exceeding specified critical spacecraft rotation rates and associated g levels. Furthermore, by assuming that the number of exceedances of rotation rate and induced gravity during an orbital experiment with duration time T are Poisson processes, estimates of the risk associated with exceeding specified critical rotation rate and induced gravity levels at least once during an experiment are obtained. It should be remembered that the calculations presented are speculative in nature and must await statistical analyses of results from Monte Carlo simulations and/or of space vehicle acceleration data acquired from previous orbital missions. However, it is believed that the calculations presented are interesting and thought provoking and may be useful to scientists and technologists who are developing space flight experiments which are sensitive to space vehicle accelerations.

II. SPACECRAFT MOTION DESCRIPTION

Let us consider a body-fixed frame of reference located at the spacecraft center of mass. This orthogonal frame of reference is fixed to the spacecraft with the x, y, and z axes directed along the principal axes of the spacecraft. Let us now consider a fluid container with center of mass located at position vector $\vec{r}_f$ with components x_f, y_f, and z_f relative to the spacecraft center of mass. Furthermore, assume the container is rigidly attached to the vehicle. If the vehicle undergoes rotation, then a fluid particle located at position $\vec{r}_o$ with respect to the spacecraft center of mass with components x_o, y_o, and z_o will experience a force per unit mass in response to the vehicle motion in question which is given by

$$\vec{F} = \dot{\vec{\Omega}} \times \vec{r}_f + \vec{\Omega} \times (\vec{\Omega} \times \vec{r}_f) - 2\vec{\Omega} \times \vec{u}(r_f', t) + \vec{a} \quad , \tag{1}$$

where $\vec{a}$ is the inertial linear acceleration of the vehicle instantaneous center of mass resulting from a net force acting on the vehicle, $\vec{\Omega}$ is the rotation vector of the vehicle with components Ω_x, Ω_y, and Ω_z directed along the principal axes of the spacecraft, and $(\dot{\vec{\Omega}})$ denotes differentiation with respect to time [3]. The vector quantity $\vec{u}(\vec{r}_f', t)$ is the velocity vector of the fluid particle with position vector $\vec{r}_f'$ relative to a frame of reference with coordinates x', y', and z' located at the fluid container center of mass and is fixed relative to the fluid container walls so that

$$\vec{r}_f = \vec{r}_f' + \vec{r}_o \quad . \tag{2}$$

Figure 1 depicts the various frames of reference and the position vectors $\vec{r}_o$, $\vec{r}_f$, and $\vec{r}_f'$. If the spatial extent of the fluid mass is small compared to the distance between the centers of mass of the spacecraft and the fluid container (i.e., $|\vec{r}_f'| << |\vec{r}_o|$), equation (1) may be written as

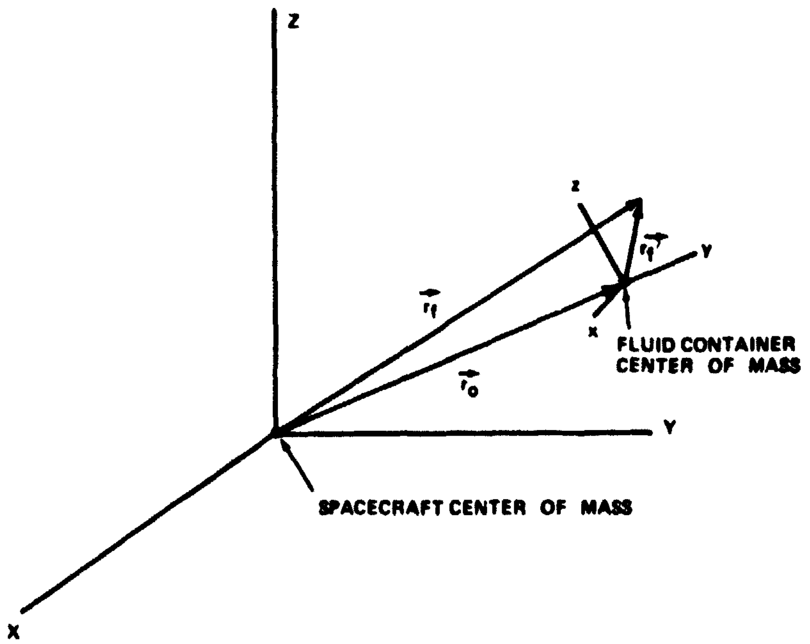

Figure 1. Principal axis and fluid container reference frames.

$$\vec{F} = \dot{\vec{\Omega}} \times \vec{r}_o + \vec{\Omega} \times (\vec{\Omega} \times \vec{r}_o) + \vec{a} - 2\vec{\Omega} \times \vec{u}(\vec{r}_f{}', t) \quad . \tag{3}$$

The first three terms on the right side of equation (3) can be treated as a time-dependent gravitational body force per unit mass. The third term is a Coriolis force. Our analysis will be concerned with statistical definition of the gravitational-like body force terms in equation (3) (excluding the linear acceleration term)

$$\vec{g}(t) = \dot{\vec{\Omega}} \times \vec{r}_o + \vec{\Omega} \times (\vec{\Omega} \times \vec{r}_o) \tag{4}$$

and the angular velocity vector $\vec{\Omega}$. It should be noted that if the fluid container is rotating (in addition to any rotations that may be imparted by the spacecraft), then precessional fluid flow analysis may be required, thus invalidating equations (3) and (4). This case is not treated in this report.

The analysis of the statistics of $\vec{g}(t)$ with the linear acceleration term included increases the complexity of the analysis. The more general case in which induced gravity results from both rotational and linear accelerations will be analyzed in a subsequent report.

The approximation $\vec{r}_f \approx \vec{r}_o$ is extremely important because this approximation means that the gravitational body force which acts on a fluid particle due to spacecraft rotations can be specified a priori in the sense that $\vec{g}$ to a sufficient degree of approximation is independent of the fluid flow dependent variables. If $\vec{r}_f$ cannot be approximated with $\vec{r}_o$, then $\vec{g}$ cannot be specified *a priori* because $\vec{r}_f$ is a fluid particle Lagrangian position vector which must then be determined as part of the fluid mechanics problem in question.

A. Spacecraft Equations

To develop the connection between the dynamics of the spacecraft and the vector quantities $\vec{g}$ and $\dot{\vec{\Omega}}$, the rigid-body equations of motions for the spacecraft referenced to the principal axes are used. These equations, in vector notation, are given by

$$\tilde{I} \cdot \dot{\vec{\Omega}} = \vec{T} + (\vec{\Omega} \cdot \tilde{I}) \times \vec{\Omega} \quad , \tag{5}$$

where $\vec{T}$ is the net torque that acts on the spacecraft and $\tilde{I}$ is the moment of inertia tensor with diagonal values I_x, I_y, and I_z and zeroes for the off-diagonal values [1].

B. Linearized Equations

The torque $\vec{T}$ results from rocket thruster firings and crew activity. Some of the forces associated with crew activity (e.g., push-offs, bending, instrument operation, etc.) have been quantified during Skylab missions and are documented in Reference 2. It appears that crew activity results in vehicle rotation with time scales on the order of seconds to a few tens of seconds. In our analysis, we shall be concerned with rocket thruster firing inputs required to keep a vehicle in a certain attitude in response to vehicle motions resulting from crew motions. These rocket firings produce relatively short period variability in $\vec{\Omega}$ and hence in $\vec{g}$. Rocket firings associated with major changes in vehicle attitude will not be included in our analysis. Therefore, the terms involving products of rotation rates in equations (4) and (5) may be neglected relative to the terms involving derivatives of rotation rates. It will be assumed that this is permissible and the following equations for $\vec{\Omega}$ and $\vec{g}$ will be used in the subsequent analysis:

$$\tilde{I} \cdot \dot{\vec{\Omega}} = \vec{T} \quad , \tag{6}$$

$$\vec{g} = \dot{\vec{\Omega}} \times \vec{r}_o \quad . \tag{7}$$

The validity of the decision to neglect the second-order terms involving $\vec{\Omega}$ to obtain these equations should be examined for each situation. The linearization process used to obtain equation (6) does not include the possible dependence of $\vec{T}$ upon a control law and, in turn, a dependence of the control law upon $\vec{\Omega}$. We shall bypass this issue by assuming that the statistics of $\vec{T}$ are known so that a statistical model of $\vec{\Omega}$ and $\vec{g}$ can be developed via a rotational approach with equations (6) and (7).

The use of equation (5) as a model to represent the combined effects of crew motion and rocket thrusters on spacecraft attitude is presumptuous. A model which includes crew motion exactly would be extremely complex because equations of motion for the vehicle and the crew members would be required. These equations would include the effects of crew members attaching and detaching from the vehicle; vehicle crew member push-offs, sneezing, etc., stochastic location of the crew members in time; and a host of other effects. An equation such as equation (5) would result from an analysis where $\vec{\Omega}$ would be the rotation rate of the vehicle about the vehicle center of mass (without crew), $\tilde{I}$ would be the moment of inertia tensor of the vehicle (without crew), and $\vec{T}$ would contain the crew member/spacecraft coupling terms and the torques imparted by the rocket thrusters. Equation (5) together with additional equations governing the crew would then require simultaneous solution for the dynamic dependent variables of the crew and spacecraft. Thus, equation (5) should be viewed as an extremely simplified model of a complex system. However, it should be noted that equation (5) is exact for the problem of calculating the response statistics of spacecraft motions resulting from stochastically imposed torques for a constant moment of inertia vehicle.

It can be shown for spacecraft such as the Space Shuttle Orbiter with Spacelab as a payload that to neglect the terms in equations (4) and (5) which are second order in $\vec{\Omega}$, we must require the lowest characteristic frequency ω_f of the random process $\vec{\Omega}$ to be very large compared to any component of $\vec{\Omega}$; i.e.,

$$\frac{\omega_f}{\Omega_x}\ ,\ \frac{\omega_f}{\Omega_y}\ ,\ \frac{\omega_f}{\Omega_z} \gg 1 \quad . \tag{8}$$

Typically, $\Omega_x, \Omega_y, \Omega_z \lesssim 0.01$ rad sec^{-1} for Spacelab missions 1 and 3 [3]. Furthermore, crew activity and rocket thruster firings produce vehicle rotations with time scales on the order of seconds to tens of seconds or, rather, frequencies $\omega \gtrsim 0.1$ rad sec^{-1}, so that $\omega_f \approx 0.1$ rad sec^{-1} and $\omega_f/\Omega_{x,y,z} \approx 10$. If we accept 10 as being large compared to unity, then equation (8) appears to be satisfied for the application intended in this report.

C. Stochastic Models

In this section we develop a stochastic model for $\vec{\Omega}$ and $\vec{g}$ based on equations (6) and (7) and as assumed stochastic model for $\vec{T}$.

1. Torque Stochastic Model. We hypothesize that the components of the torque vector are mutually uncorrelated, statistically stationary Gaussian processes which have zero mean values and spectral density functions given by

$$\left.\begin{aligned} \phi_{T_x,T_x}(\omega) &= \frac{\sigma^2_{T_x,T_x}}{2(\omega_o - \omega_1)} \ , \ \omega_1 < |\omega| < \omega_o \\ \phi_{T_x,T_x}(\omega) &= 0 \ , \ 0 < |\omega| < \omega_1 \ , \ \text{or} \ \omega_o < |\omega| < \infty \end{aligned}\right\} \ , \tag{9}$$

with similar equations assumed for T_y and T_z. The quantity ω is radian frequency (Paragraph II.C.2), σ_{T_x,T_x} is the standard deviation of T_x, and ω_o and ω_1 are upper and lower bound frequencies, respectively. The spectrum in equation (9) and all those that follow in the subsequent development are defined such that integration over the domain $-\infty < \omega < \infty$ yields the auto- or cross-variance. The assumption that the components of the torque vector are uncorrelated appears to be reasonable for the crew activity contribution to torque. However, this assumption may not be true for the thruster firing contribution to the torque vector. Nevertheless, this assumption is used in the analysis which follows.

2. Rotation Vector Stochastic Process. We express $\vec{\Omega}$ and $\vec{T}$ in terms of Fourier-Steltjes integrals [4]

$$\vec{\Omega}(t) = \int_{-\infty}^{\infty} e^{i\omega t} \, d\hat{\vec{\Omega}}(\omega) \quad , \tag{10}$$

$$\vec{T}(t) = \int_{-\infty}^{\infty} e^{i\omega t}\, d\hat{\vec{T}}(\omega) \quad , \tag{11}$$

where t is time and $d\vec{\xi}(\omega)$ denotes stochastic Fourier amplitude at frequency ω of the random process $\vec{\xi}(t)$. Substituting equations (10) and (11) into equation (6) yields the Fourier amplitudes of the $\vec{\Omega}$ process. For the x component, we have

$$d\hat{\Omega}_x(\omega) = \frac{d\hat{T}_x(\omega)}{i\omega I_x} \quad , \tag{12}$$

with similar equations for the y and z component rigid-body equations. Multiplying equation (12) by its complex conjugate evaluated at frequency ω' and applying the ensemble average operator over all realizations of the $(\vec{\Omega},\vec{T})$ process yields

$$\left\langle d\hat{\Omega}_x(\omega)\; d\hat{\Omega}_x^*(\omega')\right\rangle = \frac{\left\langle d\hat{T}_x(\omega)\; d\hat{T}_x^*(\omega')\right\rangle}{\omega\omega' I_x^2} \quad , \tag{13}$$

where the asterisk denotes complex conjugation and the angular brackets denote the ensemble average operator. The requirement of statistical orthogonality of Fourier components or statistical stationarity of a random process in the time domain demands that

$$\left\langle dA(\omega)\; dB^*(\omega')\right\rangle = \begin{cases} \phi_{A,B}(\omega)\, d\omega & \text{if } \omega = \omega' \\ 0 & \text{if } \omega \neq \omega' \, , \end{cases} \tag{14}$$

where $\phi_{A,B}(\omega)$ is a spectral density function [4]. Thus, equation (11) reduces to

$$\phi_{\Omega_x,\Omega_x}(\omega) = \frac{\phi_{T_x,T_x}(\omega)}{\omega^2 I_x^2} \quad . \tag{15}$$

Combining equations (9) and (15) yields

$$\begin{aligned} \phi_{\Omega_x,\Omega_x}(\omega) &= \frac{\sigma^2_{T_x,T_x}}{2I_x^2(\omega_o - \omega_1)\,\omega^2} \quad , \quad \omega_1 < |\omega| \le \omega_o \\ \phi_{\Omega_x,\Omega_x}(\omega) &= 0 \quad , \quad 0 < |\omega| \le \omega_1 \quad \text{or} \quad \omega_o < |\omega| \quad . \end{aligned} \tag{16}$$

This result states that $\phi_{\Omega_x,\Omega_x}(\omega) \propto \omega^{-2}$ over the frequency domain in which $\phi_{T_x,T_x}(\omega)$ takes on nonzero values. Equations similar to equation (16) can be written for Ω_y and Ω_z.

If it is assumed that the components of the torque vector are uncorrelated, it follows that the cross-spectral density functions of the components of $\vec{\Omega}$ vanish so that

$$\phi_{\Omega_x,\Omega_y}(\omega) = \phi_{\Omega_x,\Omega_y}(\omega) = \phi_{\Omega_y,\Omega_z}(\omega) = 0 \quad , \quad -\infty < \omega < \infty \quad . \tag{17}$$

Statistical stationarity demands that the ensemble mean $\langle\vec{\Omega}\rangle$ be equal to a constant vector $\vec{\Omega}_o$. Thus $\langle\dot{\vec{\Omega}}\rangle = 0$, which means $\langle\vec{T}\rangle = 0$ as hypothesized *ab initio*. For definiteness we shall set $\vec{\Omega}_o = 0$.

Integrating equation (16) over the domain $-\infty < \omega < \infty$ yields the variance of Ω_x; i.e.,

$$\sigma^2_{\Omega_x,\Omega_x} = \frac{\sigma^2_{T_x,T_x}}{I_x^2\,\omega_o^2\,\beta} \quad , \tag{18}$$

where $\beta = \omega_1/\omega_o$. Similar equations can be obtained for the remaining components of $\vec{\Omega}$.

In view of the linear relationship between $\vec{\Omega}$ and $\vec{T}$ as expressed by equation (6) and the assumed Gaussian nature of the torque process, it follows that $\vec{\Omega}$ is a Gaussian vector process. The previously mentioned data concerning the moments of the $\vec{\Omega}$ process provide sufficient information to determine any desired probability density function of the components of $\vec{\Omega}$ and hence to calculate any desired statistic of the $\vec{\Omega}$ process.

3. <u>Body Force Vector Stochastic Process</u>. The Fourier-Steltjes stochastic decomposition of $\vec{g}(t)$ is expressed mathematically as

$$\vec{g}(t) = \int_{-\infty}^{\infty} e^{i\omega t}\, d\hat{\vec{g}}(\omega) \quad . \tag{19}$$

Substituting equations (10) and (19) into equation (7) yields

$$d\hat{\vec{g}}(\omega) = d\hat{\dot{\vec{\Omega}}} \times \vec{r}_o \quad . \tag{20}$$

Application of the ensemble average operator to equation (20) (noting that $\langle\dot{\vec{\Omega}}\rangle = 0$ and hence $\langle d\hat{\dot{\vec{\Omega}}}\rangle = 0$) yields $\langle d\hat{\vec{g}}(\omega)\rangle = 0$ and hence $\langle\vec{g}(t)\rangle = 0$. Thus, the ensemble mean body force is zero in this model.

Following the procedure outlined in Paragraph II.C.2, the following spectral density functions are obtained:

$$\phi_{g_x,g_x}(\omega) = \omega^2\left[z_o^2\,\phi_{\Omega_y,\Omega_y}(\omega) + y_o^2\,\phi_{\Omega_z,\Omega_z}(\omega)\right] \quad . \tag{21}$$

$$\phi_{g_y,g_y}(\omega) = \omega^2\left[x_o^2\,\phi_{\Omega_z,\Omega_z}(\omega) + z_o^2\,\phi_{\Omega_x,\Omega_x}(\omega)\right] \quad , \tag{22}$$

$$\phi_{g_z,g_z}(\omega) = \omega^2\left[y_o^2\,\phi_{\Omega_x,\Omega_x}(\omega) + x_o^2\,\phi_{\Omega_y,\Omega_y}(\omega)\right] \quad , \tag{23}$$

$$\phi_{g_y,g_x}(\omega) = \phi_{g_x,g_y}(\omega) = -x_o\,y_o\,\omega^2\,\phi_{\Omega_z,\Omega_z}(\omega) \quad , \tag{24}$$

$$\phi_{g_z,g_x}(\omega) = \phi_{g_x,g_z}(\omega) = -x_o\,z_o\,\omega^2\,\phi_{\Omega_y,\Omega_y}(\omega) \quad , \tag{25}$$

$$\phi_{g_z,g_y}(\omega) = \phi_{g_y,g_z}(\omega) = -y_o\,z_o\,\omega^2\,\phi_{\Omega_x,\Omega_x}(\omega) \quad . \tag{26}$$

Substituting the rotation rate spectral density functions into equations (21) through (26) yields

$$\left.\begin{aligned}
\phi_{g_x,g_x}(\omega) &= \frac{\sigma^2_{g_x,g_x}}{2(\omega_o - \omega_1)} \quad , \quad \omega_1 < |\omega| \le \omega_o \\
\phi_{g_x,g_x}(\omega) &= 0 \quad , \quad 0 < |\omega| \le \omega_1 \quad \text{or} \quad \omega_o < |\omega|
\end{aligned}\right\} \quad , \tag{27}$$

with similar equations for g_y and g_z and

$$\sigma^2_{g_x,g_x} = \frac{z_o^2\,\sigma^2_{T_y,T_y}}{I_y^2} + \frac{y_o^2\,\sigma^2_{T_z,T_z}}{I_z^2} \quad , \tag{28}$$

$$\sigma^2_{g_y,g_y} = \frac{x_o^2\,\sigma^2_{T_z,T_z}}{I_z^2} + \frac{z_o^2\,\sigma^2_{T_x,T_x}}{I_x^2}\quad , \tag{29}$$

$$\sigma^2_{g_z,g_z} = \frac{y_o^2\,\sigma^2_{T_x,T_x}}{I_x^2} + \frac{x_o^2\,\sigma^2_{T_y,T_y}}{I_y^2}\quad , \tag{30}$$

$$\begin{aligned}
\phi_{g_y,g_x}(\omega) = \phi_{g_x,g_y}(\omega) &= -\frac{\sigma^2_{g_x,g_y}}{2(\omega_o - \omega_1)}\ , \quad \omega_1 < |\omega| < \omega_o\ , \\
\phi_{g_y,g_x}(\omega) = \phi_{g_x,g_y}(\omega) &= 0\ , \quad 0 < |\omega| < \omega_1 \ \text{ or } \ \omega_o < |\omega|\ ,
\end{aligned} \tag{31}$$

with similar equations for the remaining cross-spectral densities and

$$\sigma^2_{g_y,g_x} = \sigma^2_{g_x,g_y} = -\frac{x_o\,y_o}{I_z^2}\,\sigma^2_{T_z,T_z}\ , \tag{32}$$

$$\sigma^2_{g_z,g_x} = \sigma^2_{g_x,g_z} = -\frac{x_o\,z_o}{I_y^2}\,\sigma^2_{T_y,T_y}\ , \tag{33}$$

$$\sigma^2_{g_z,g_y} = \sigma^2_{g_y,g_z} = -\frac{y_o\,z_o}{I_x^2}\,\sigma^2_{T_x,T_x}\ . \tag{34}$$

Because of the linear relationship between $\vec{g}$ and $\vec{\Omega}$ [as expressed by equation (7)] and because $\vec{\Omega}$ is a Gaussian process, it follows that $\vec{g}$ is a Gaussian vector process. The previously mentioned data concerning the moments of the g process provide sufficient information to determing any desired probability density function of the components of $\vec{g}$ and hence to calculate any desired statistic of the $\vec{g}$ process.

Since the $\vec{g}$ process is Gaussian, there exists an orthogonal transformation of the spacecraft principal axis reference frame (x, y, z) to a new frame of reference (X, Y, Z) such that the cross correlations of the components of $\vec{g}$ in the (X, Y, Z) frame vanish [5]. The components of $\vec{g}$ referenced to the (X, Y, Z) frame are stochastically independent Gaussian processes. The transformation of the $\vec{g}$ process referenced in the (x, y, z) frame [i.e., $\vec{g}(t;x,y,z)$] to the (X, Y, Z) frame [i.e., $\vec{g}(t;X,Y,Z)$] is given by

$$\vec{g}(t;X,Y,Z) = \tilde{A} \cdot \vec{g}(t;x,y,z) \quad , \tag{35}$$

where $\tilde{A}$ is a 3 by 3 tensor with components that are functions of the auto- and cross-covariances of the $\vec{g}$ process referenced to the (x, y, z) frame, i.e., equations (28), (29), (30), (32), (33), and (34). The components of $\tilde{A}$ can be determined by a relatively straightforward application of a three-way Euler angle transformation [3] subject to the constraint that

$$\sigma^2_{g_X,g_Y} = \sigma^2_{g_Z,g_X} = \sigma^2_{g_Z,g_Y} = 0 \quad . \tag{36}$$

Upon determination of the components of $\tilde{A}$, the spectral density functions of $\vec{g}(t;X,Y,Z)$ can be obtained by Fourier transformation of equation (35) and formation of the appropriate square modulii. Thus, for example, Fourier transformation of $\vec{g}_X$ yields

$$d\hat{g}_X = A_{xx} d\hat{g}_x(\omega) + A_{xy} d\hat{g}_y(\omega) + A_{xz} d\hat{g}_z(\omega) \quad . \tag{37}$$

Multiplying equation (37) by its complex conjugate at frequency ω' and applying the condition of statistical orthogonality [equation (14)] yields

$$\phi_{g_X, g_X}(\omega) = A_{xx}^2 \phi_{g_x, g_x}(\omega) + 2A_{xx}A_{xy} \phi_{g_x, g_y}(\omega)$$

$$+ 2A_{xx}A_{xz} \phi_{g_x, g_z}(\omega) + A_{xy}^2 \phi_{g_y, g_y}(\omega)$$

$$+ 2A_{xy}A_{xz} \phi_{g_y, g_z}(\omega) + A_{xz}^2 \phi_{g_z, g_z}(\omega) \quad . \tag{38}$$

Thus, the spectral density function of $\vec{g}(t;X,Y,Z)$ can be calculated directly from the spectral density functions of $\vec{g}(t;x,y,z)$. The cross-spectral density functions of $\vec{g}(t;X,Y,Z)$ vanish identically. The main point that we want to make is that there exists a coordinate system such that the components of $\vec{g}$ in that frame of reference are stochastically independent and that the statistics of $\vec{g}(t;X,Y,Z)$ are derivable from the statistics of $\vec{g}(t;x,y,z)$.

The spectral density functions of $\vec{g}(t;X,Y,Z)$ are of the form

$$\phi_{g_X, g_X}(\omega) = \frac{\sigma^2_{g_X, g_X}}{2(\omega_o - \omega_1)} \quad , \quad \omega_1 < |\omega| < \omega_o \quad ,$$

$$\phi_{g_X, g_X}(\omega) = 0 \quad , \quad 0 < |\omega| < \omega_1 \quad \text{or} \quad \omega_o < |\omega| \quad , \tag{39}$$

where

$$\sigma^2_{g_X, g_X} = A_{xx}^2 \sigma^2_{g_x, g_x} + 2A_{xx}A_{xy} \sigma^2_{g_x, g_y} + 2A_{xx}A_{xz} \sigma^2_{g_x, g_z}$$

$$+ A_{xy}^2 \sigma^2_{g_y, g_y} + 2A_{xy}A_{xz} \sigma^2_{g_y, g_z} + A_{xz}^2 \sigma^2_{g_z, g_z} \quad . \tag{40}$$

Similar expressions can be obtained for the Y and Z components of $\vec{g}$.

4. <u>Cross Correlations of the Rotation and Body Force Vector Processes.</u> The fact that $\vec{g}$ is derived from $\vec{\Omega}$ implies a correlation between the $\vec{g}$ process with the $\vec{\Omega}$ process. The following cross-spectral density functions can be calculated from equation (20):

$$\phi_{g_x,\Omega_x}(\omega) = \phi_{\Omega_x,g_x}(\omega) = 0 \quad . \tag{41}$$

$$\phi_{g_y,\Omega_y}(\omega) = \phi_{\Omega_y,g_y}(\omega) = 0 \quad . \tag{42}$$

$$\phi_{g_z,\Omega_z}(\omega) = \phi_{\Omega_z,g_z}(\omega) = 0 \quad . \tag{43}$$

$$\phi_{g_x,\Omega_y}(\omega) = \phi^*_{\Omega_y,g_x}(\omega) = i\omega z_o\,\phi_{\Omega_y,\Omega_y}(\omega) \quad , \tag{44}$$

$$\phi_{g_x,\Omega_z}(\omega) = \phi^*_{\Omega_z,g_x}(\omega) = -i\omega y_o\,\phi_{\Omega_z,\Omega_z}(\omega) \quad . \tag{45}$$

$$\phi_{g_y,\Omega_x}(\omega) = \phi^*_{\Omega_x,g_y}(\omega) = -i\omega z_o\,\phi_{\Omega_x,\Omega_x}(\omega) \quad . \tag{46}$$

$$\phi_{g_y,\Omega_z}(\omega) = \phi^*_{\Omega_z,g_y}(\omega) = i\omega x_o\,\phi_{\Omega_z,\Omega_z}(\omega) \quad . \tag{47}$$

$$\phi_{g_z,\Omega_x}(\omega) = \phi^*_{\Omega_x,g_z}(\omega) = i\omega y_o\,\phi_{\Omega_x,\Omega_x}(\omega) \quad . \tag{48}$$

$$\phi_{g_z,\Omega_y}(\omega) = \phi^*_{\Omega_y,g_z}(\omega) = -i\omega x_o\,\phi_{\Omega_y,\Omega_y}(\omega) \quad . \tag{49}$$

Equations (41) through (43) show that parallel components of $d\hat{\vec{\Omega}}$ and $d\hat{\vec{g}}$ are uncorrelated, so that parallel components of $\vec{g}$ and $\vec{\Omega}$ are uncorrelated. The cross-spectral densign functions of the mutually orthogonal components of $\vec{g}$ and $\vec{\Omega}$ are complex according to equations (44) through (49). This means the mutually orthogonal components of $\vec{g}$ and $\vec{\Omega}$ are out of phase by ±90 deg. Thus, for example, the Fourier components of Ω_y lead those of g_x by 90 deg. Integrating equations (38) through (43) over the domain $-\infty < \omega < \infty$ yields

$$\sigma^2_{g_x,\Omega_y} = \sigma^2_{\Omega_y,g_x} = 0 \ , \tag{50}$$

and likewise for the remaining cross correlations between the mutually orthogonal components of $\vec{g}$ and $\vec{\Omega}$. These results show that $\vec{g}(t)$ is uncorrelated with $\vec{\Omega}(t)$! The $\vec{g}$ and $\vec{\Omega}$ processes are, however, correlated for finite nonzero time delay τ. This can be shown by the Fourier transformation of equations (44) through (49) to the τ domain to obtain the cross-correlation function $R(\tau)$ between the mutually orthogonal components of $\vec{g}(t+\tau)$ and $\vec{\Omega}(t)$. Thus, for example,

$$R_{g_x,\Omega_y}(\tau) = \frac{1}{2\pi}\int_{-\infty}^{\infty} e^{i\omega\tau}\,\phi_{g_x,\Omega_y}(\omega)\,d\omega$$

$$= -\frac{1}{2\pi}\frac{z_o\,\sigma^2_{T_y,T_y}}{I_x^2\,(\omega_o-\omega_1)}\int_{\omega_1\tau}^{\omega_o\tau}\frac{\sin\xi}{\xi}\,d\xi \ , \tag{51}$$

where the sine integral is tabulated in standard references. Thus, for $\tau \neq 0$, $R_{g_x,\Omega_y}(\tau) \neq 0$, with similar results for the remaining cross-correlation functions between the orthogonal components of $\vec{g}$ and $\vec{\Omega}$.

III. BODY FORCE PROCESS EXCEEDANCE STATISTICS

In this section we determine the exceedance statistics of each component of the $\vec{g}$ process referenced to the (X, Y, Z) frame discussed in Paragraph II.C.3. Our analysis will be concerned with a single component of $\vec{g}$; consequently, we will dispense with subscripts on g to denote components. We will use the symbol g to denote a component of $\vec{g}$ and σ_g to denote the standard deviation of g.

A. Rice's Theorem and Expected Exceedance Rate of Body Force

According to Rice [6, 7], for a stationary Gaussian process with zero mean, the expected number of exceedances of induced gravity per unit time which exceed level g is given by

$$N_g = N_{g,o}\, e^{-g^2/2\sigma_g^2} \quad . \tag{52}$$

The quantity $N_{g,o}$ is the expected number of zero crossings of the quantity g from below and is related to the spectral density function $\phi_g(\omega)$ through the following expression:

$$N_{g,o} = \frac{1}{2\pi}\left\{\frac{\int_{-\infty}^{\infty} \omega^2\, \phi_g(\omega)\, d\omega}{\sigma_g^2}\right\}^{1/2} \quad . \tag{53}$$

Thus, the substitution of equation (39) into equation (52) yields for our assumed stochastic g process

$$N_{g,o} = \frac{\omega_o}{2\pi}\left(\frac{1-\beta^3}{3(1-\beta)}\right)^{1/2} \quad , \tag{54}$$

where $\beta = \omega_1/\omega_o$. The quantity β serves as a relative measure of the spectral bandwidth of the g jitter process. For a relatively broad-banded process in which $\beta = 0$, $2\pi N_{g,o}/\omega_o = 3^{-1/2}$; and for a narrow process in which $\beta \to 1$, we have $2\pi N_{g,o}/\omega_o = 1$. If the process were characterized by a monochromatic spectral density function, namely

$$\phi(\omega) = \sigma_g^2 \left[\frac{\delta(\omega - \omega_o) + \delta(\omega + \omega_o)}{2} \right] . \tag{55}$$

where $\delta(\ )$ is the Dirac delta function, then the zero-crossing rate would be given by $N_o = \omega_o/2\pi$ as calculated for $\beta = 1$ with the g jitter spectral model given by equation (39). Thus, the model given by equation (39) includes broad-banded and narrow-banded g jitter processes with the limiting case of monochromatic g jitter.

Substituting equation (54) into equation (52) yields

$$\frac{2\pi N_g}{\omega_o} = \left[\frac{1 + \beta + \beta^2}{3} \right]^{1/2} e^{-g^2/2\sigma_g^2} . \tag{56}$$

The nondimensional exceedance rate $2\pi N_g/\omega_o$ is plotted in Figure 2 as a function of g/σ_g for $\beta = 0$ and $\beta = 0.999$. Thus, we conclude from Figure 2 that for any given value of g/σ_g the exceedance rate will vary by only a factor of 1.733 over the admissible range of β. This means that for the model selected the exceedance rate N_g of the g process is only mildly dependent on the parameter β. The dependence of N_g on β occurs through the zero-crossing rate $N_{g,o}$ [equation (54)] and, as previously noted, $3^{-1/2} \le 2\pi N_{g,o}/\omega_o \le 1$

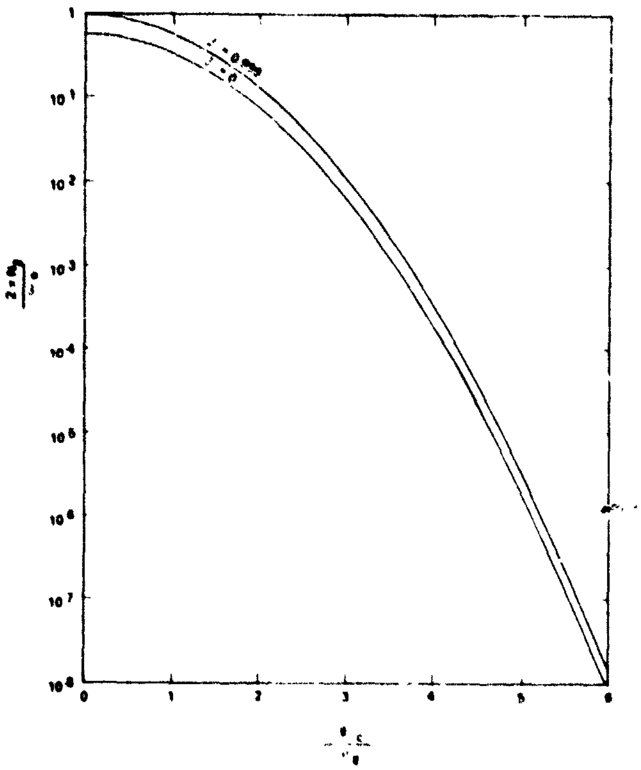

Figure 2. Nondimensional expected rate $2\pi N_g/\omega_o$ of exceeding the nondimensional level $|g|_c/\sigma_g$ with positive slope for $g > 0$ or negative slope for $g < 0$. (The expected rate of exceeding level $|g|_c/\sigma_g$ with positive or negative slope is $2N_g$.)

for the full range of variation of the parameter β; i.e., $0 \leq \beta \leq 1$. Thus, for example, if the g process has an upper-bound frequency of $\omega_o = 2\pi$ rad sec^{-1}, then we have for the expected zero-crossing rate $0.577 \lesssim N_{g,o} \leq 1$ sec^{-1}.

It should be noted that the g process can exceed critical values of $|g|$ when $g < 0$ with negative slope; consequently, the rate at which the g process excee' a critical value is $2N_g$.

B. Risk of Body Force Exceeding a Critical Value

We now seek to determine the risk that the g process will exceed a critical value for a given orbital experiment duration time. Clearly, the larger the duration time T of an experiment, the higher the risk a critical value of $|g|$ ($|g|_c$) will be exceeded. Ideally, we wish to know the probabilistic structure of the random time T when $|g|_c$ is exceeded. This problem is called the "first passage" problem.

As previously noted, we consider the case where g is a stationary process. Furthermore, the g process is symmetrically distributed in the positive and negative ranges, and the upper and lower bounds are also symmetrical. Thus, the probability of exceeding a critical g level, $|g|_c$, at any given instant is

$$P[\{g \geq |g|_c\} \cup \{g \leq -|g|_c\}] = 2P[g \geq |g|_c] \quad . \tag{57}$$

To estimate the risk associated with $|g| \geq |g|_c$ for a given experiment duration time T, we shall make the arbitrary assumption that the exceedances of the $|g|$ process above level $|g|_c$ arrive independently. We now denote by Q(T) the number of exceedances of $|g|$ at level $|g|_c$ over the experiment duration time T. Clearly, the process Q(T) is a Poisson process, and the probability of Q(T) being less than or equal to an assigned value (for example, q) according to Lin [8], is given by

$$P(Q(T) \leq q, T) = \frac{(\lambda T)^q}{q!} e^{-\lambda T} \quad , \tag{58}$$

where λ is a parameter. The probability of no exceedance of the g process above the critical value $|g|_c$ in time interval T follows by setting $q = 0$ in equation (58), so that

$$P(Q(T) = 0, T) = e^{-\lambda T} \quad . \tag{59}$$

By definition of the Poisson process we set

$$\lambda = 2N_g \quad . \tag{60}$$

Thus,

$$P(Q(T) = 0, T) = e^{-2N_g T} \quad . \tag{61}$$

Now, the risk R that the g process will exceed the critical value $|g|_c$ at least once during an experiment of duration time T is

$$R = 1 - e^{-2N_g T} \quad . \tag{62}$$

Eliminating the expected exceedance rate N_g between equations (56) and (62) yields

$$\frac{|g|_c}{\sigma_g} = \left\{ -2 \ln \left\{ - \left[\frac{3(1-\beta)}{1-\beta^3} \right]^{1/2} \frac{\pi \ln (1-R)}{T\omega_o} \right\} \right\}^{1/2} \quad . \tag{63}$$

This formula permits the calculation of critical g level (i.e., $|g|_c$) as a function of risk R of the quantity $|g|$ exceeding level $|g|_c$ at least once during an experiment duration time T and the g environment spectral model parameters β and ω_o. Figures 3 and 4 contain plots of $|g|_c/\sigma_g$ as a function of $T\omega_o$ for various values of risk for $\beta = 0$ and 0.999, respectively.

It may be concluded from these figures that the variability in $|g|_c$ due to variation in $\omega_o T$ and/or β decreases as R decreases.

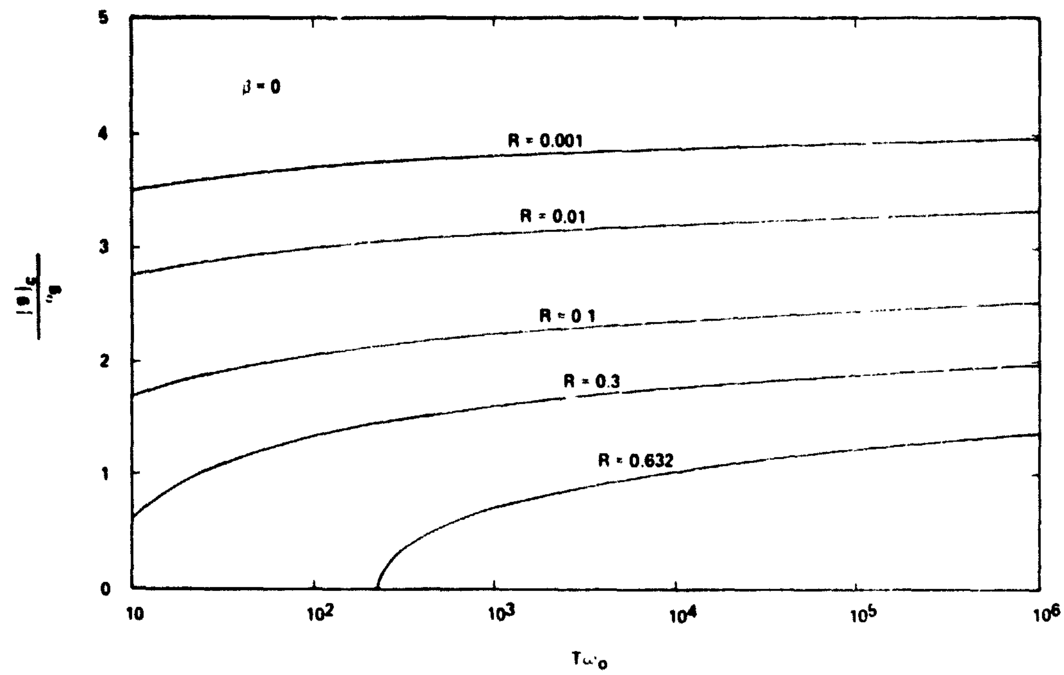

Figure 3. The quantity $|g|_c/\sigma_g$ as a function of $\omega_o T$ and R for $\beta = 0$.

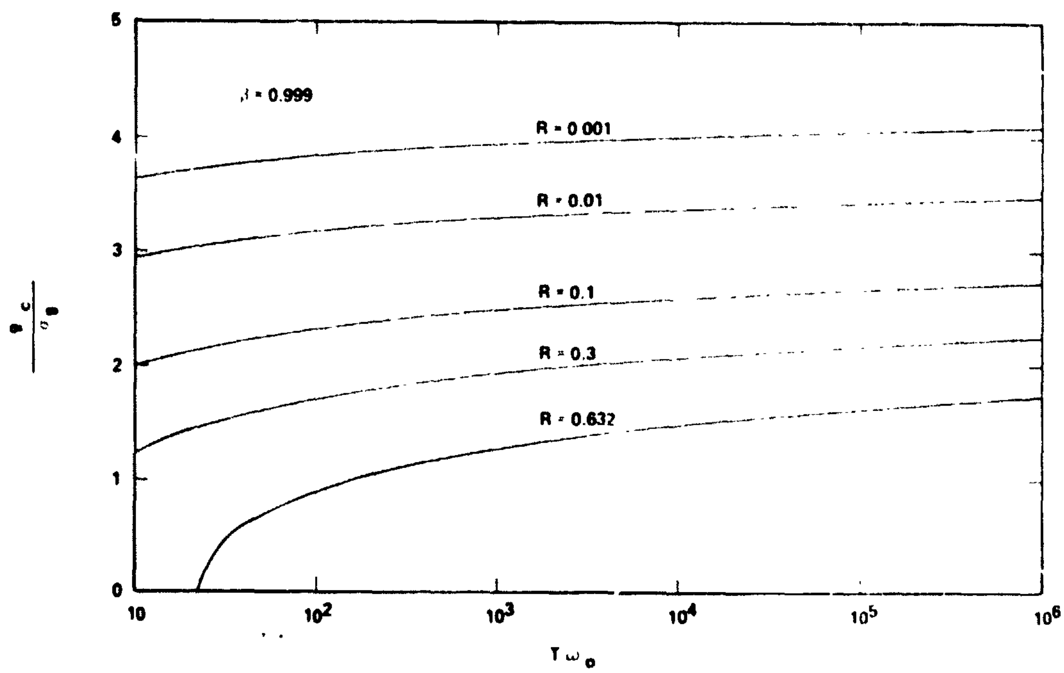

Figure 4. The quantity $|g|_c/\sigma_g$ as a function of $\omega_o T$ and R for $\beta = 0.999$.

C. Body Force Envelope Exceedance Rate

The most questionable aspect of the previous analysis is the arbitrary assumption that the arrival of the threshold crossings of g above and below the critical levels $|g|_c$ and $-|g|_c$ with positive and negative slopes, respectively, are independent events. This assumption is especially unacceptable for narrow-band g jitter because the threshold crossings of narrow-banded g jitter will tend to occur in clumps. Once there is a crossing of $|g|$ over a threshold $|g|_c$, the probability is high that the following excursion will produce another crossing. However, we note that the crossing of the same threshold by the envelope of the g process must precede the first crossing in each clump. Accordingly, when there are many excursions in each clump, the time of a threshold crossing by the envelope is nearly the same as the time of the first crossing in each clump. Thus, although it is more acceptable to treat the threshold crossings of an envelope of a narrow-banded random process as independent events, we can improve the analysis in the previous section by using the expected rate of threshold crossings of the envelope process for λ in equation (59).

From Rice [6, 7], we assume the narrow-banded g jitter process can be expressed as

$$g(t) = A(t) \cos (\omega_m t + \theta(t)) \quad , \tag{64}$$

where ω_m is a representative wide-band frequency of the g process and $A(t)$ and $\theta(t)$ are random processes which vary much more slowly than $g(t)$ with respect to t. The process $A(t)$ is nonnegative. Since the spectral density function of our assumed g jitter process is symmetric about the frequency $\omega_s = \omega_o(1 + \beta)/2$ on the half interval $0 < \omega < \infty$, it is clear that $\omega_m = \omega_s$. According to Rice, the random process $A(t)$ is the envelope process of the g process. Since the g process is Gaussian, it can be shown that the expected exceedance rate or threshold crossing rate with positive slope of the envelope of the g process at level A is given by

$$M = \frac{A}{\sigma_g} \frac{\sigma_{g,1}}{\sigma_g} \frac{1}{(2\pi)^{1/2}} e^{-A^2/2\sigma_g^2} \quad , \tag{65}$$

where

$$\sigma_{g,1}^2 = \int_{-\infty}^{\infty} (\omega^2 - \omega_m^2)\, \phi_g(\omega)\, d\omega \quad . \tag{66}$$

Substituting the g process spectral density function [equation (39)] into equation (66) yields

$$\frac{\sigma_{g,1}}{\sigma_g} = \frac{\omega_o}{(1-\beta)^{1/2}} \left\{ \frac{1-\beta^3}{3} - \frac{(1+\beta)^2 (1-\beta)}{4} \right\}^{1/2} \quad . \tag{67}$$

Furthermore, substituting equation (67) into equation (61) yields

$$\frac{2\pi M}{\omega_o} = \left\{ \frac{2\pi}{1-\beta} \left[\frac{1-\beta^3}{3} - \frac{(1+\beta)^2 (1-\beta)}{4} \right] \right\}^{1/2} e^{-A^2/2\sigma_g^2} \quad . \tag{68}$$

The nondimensional exceedance rate $2\pi M/\omega_o$ of the envelope of the g jitter process is plotted in Figure 5 as a function of A/σ_g for various values of β ranging from 0.90 to 0.999.

The values of β indicated in Figure 5 were selected such that the exceedance curve of the envelope process remains below the exceedance curve of the g jitter process (Fig. 2) for the range of values of g/σ_g and A/σ_g indicated in Figures 2 and 5, respectively. This requirement results from the fact that the exceedance rate of the envelope process should be less than the exceedance rate of the actual process at any prescribed level $g/\sigma_g = A/\sigma_g$. The fact that the theory predicts exceedance rates of the envelope process which are greater than the exceedance rates of the actual process is a result of the fact that equation (64) is strictly valid only in the limit $\beta \to 1$ (i.e., monochromatic g jitter). Equation (68) is valid only as an approximation for $\beta \neq 1$ for $A/\sigma_g > A'/\sigma_g$, where $A' > A'$. The quantity A' is defined as

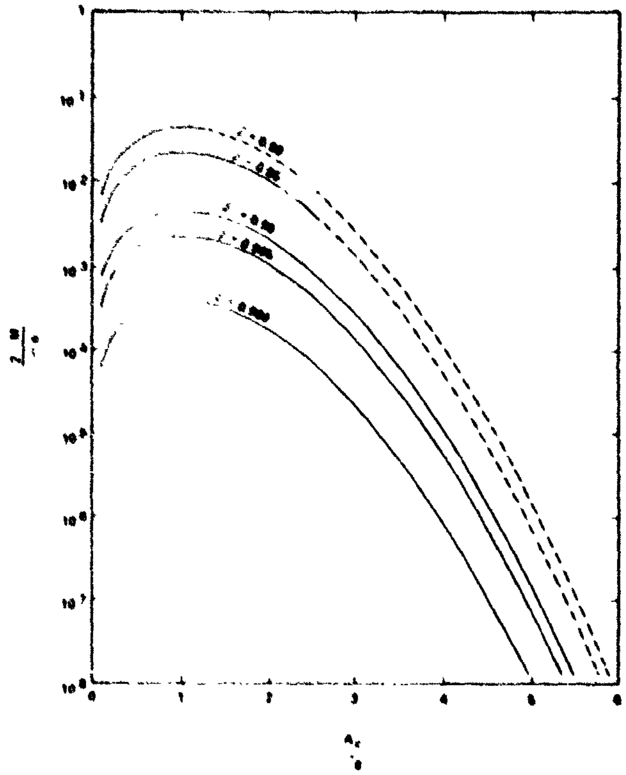

Figure 5. Nondimensional expected rate $2\pi M_g/\omega_0$ of the envelope $A(t)$ of the g jitter process exceeding level A_c/σ_g with positive slope for $g > 0$ and negative slope for $g < 0$. [The expected rate of the envelope process exceeding level A/σ_g with positive or negative slope is $2M_g$. The dashed lines correspond to the condition $A/\sigma_g > A'/\sigma_g$, equation (69).]

$$\frac{A'}{\sigma_g} = \left\{ 6\pi \left[\frac{1}{5} - \frac{(1+\beta)^2 (1-\beta)}{4(1-\beta)^3} \right] \right\}^{-1/2} \tag{69}$$

and is that value of A/σ_g such that $M_g/N_g = 1$. We shall assume that $A' = A^+/10$. The Table contains a listing of the quantity A^+/σ_g for various values of β. The dashed lines shown in Figure 5 indicate those portions of the curves for which $A/\sigma_g > A'/\sigma_g$.

TABLE. THE QUANTITY A^+/σ_g FOR VARIOUS VALUES OF β

β	A^+/σ_g
0	0.798
0.1	0.934
0.2	1.111
0.3	1.344
0.4	1.661
0.5	2.111
0.6	2.793
0.7	3.936
0.8	6.232
0.9	13.135
0.95	26.95
0.99	137.5
0.999	15544.4

D. Risk of Body Force Envelope Exceeding a Critical Value

The risk R that the envelope of the g process will exceed level A_c from below for $g > 0$ or level $-A_c$ from above for $g < 0$ at least once during the orbital experiment time T is now given by

$$R = 1 - e^{-M_g T} \quad , \tag{70}$$

where we have set $\lambda = 2M_g$. Elimination of the g jitter envelope exceedance rate between equations (65) and (68) yields

$$-\ell n(1 - R) = \omega_o T \frac{A_c}{\sigma_g} \left(\frac{2}{\pi}\right)^{1/2} \left\{\frac{1 - \beta^3}{3(1 - \beta)} - \frac{(1 + \beta)^2}{4}\right\}^{1/2} e^{-A_c^2/2\sigma_g^2} \tag{71}$$

where we have substituted for $\sigma_{g,1}/\sigma_g$ with equation (67). Figures 6 through 10 contain plots of A_c/σ_g as a function of $\omega_o T$ for various values of R and β ranging from 0.90 to 0.999. Again, the strong dependence of the statistics of the envelope process on β is reflected in these figures. It should be noted that because of the restrictions on the value of A for which the envelope exceedance analysis is valid, the parameter β was restricted to values in the interval $0.90 \leq \beta < 1$ for the construction of Figures 6 through 10.

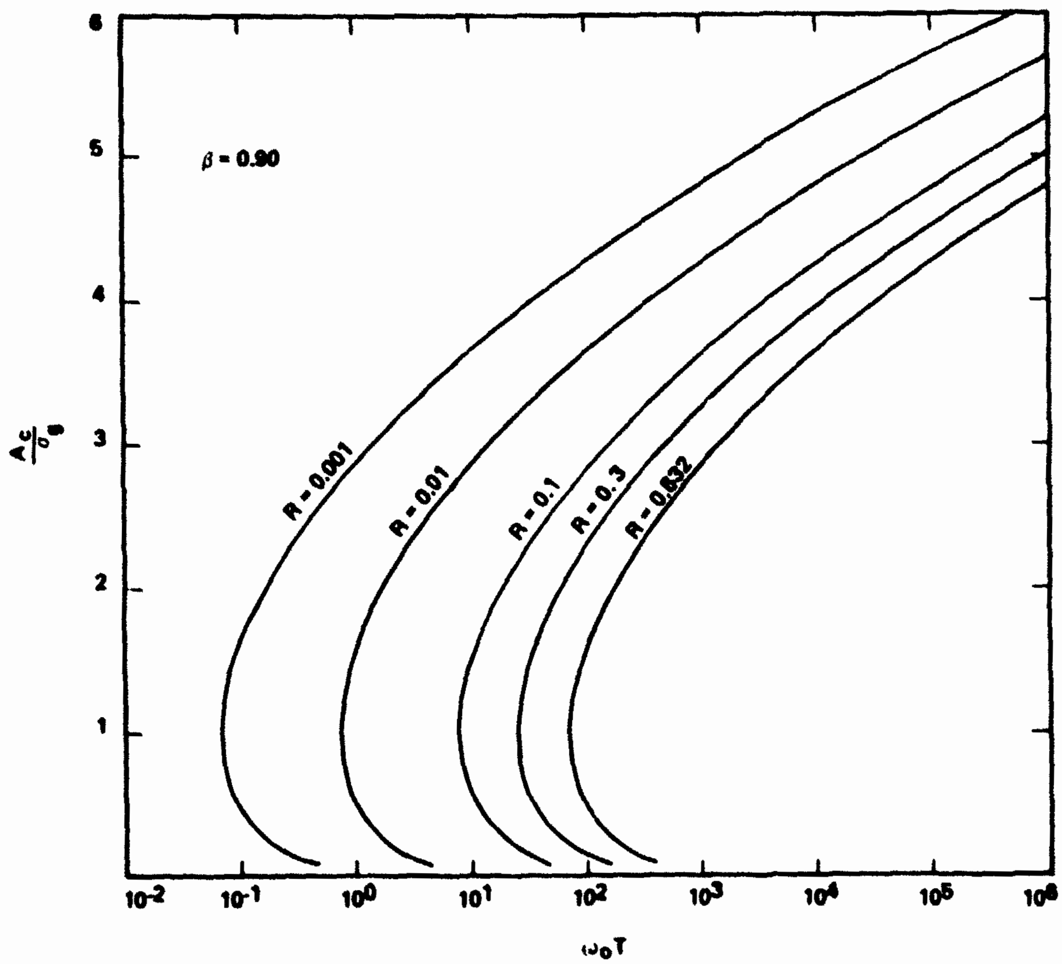

Figure 6. The quantity A_c/σ_g as a function of $\omega_o T$ and R for $\beta = 0.90$.

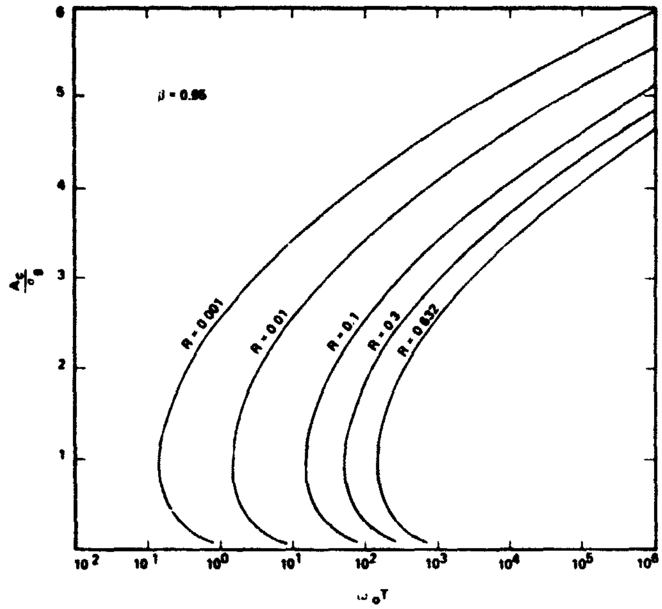

Figure 7. The quantity A_c/σ_g as a function of $\omega_o T$ and R for $\beta = 0.95$.

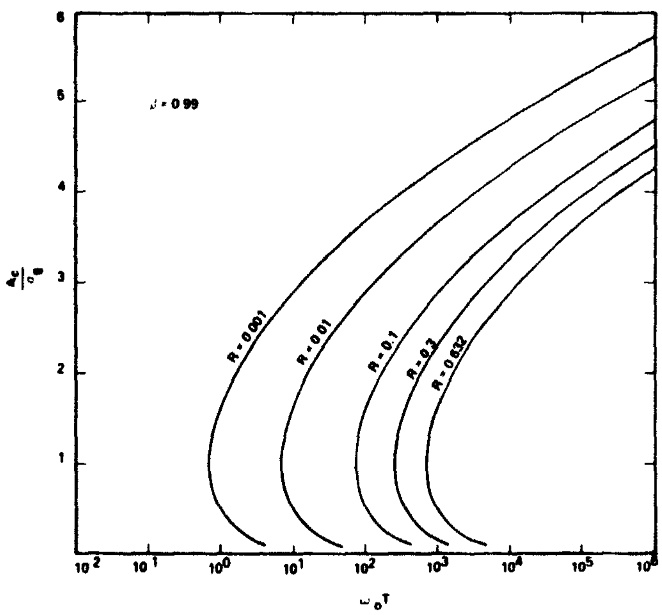

Figure 8. The quantity A_c/σ_g as a function of $\omega_o T$ and R for $\beta = 0.99$.

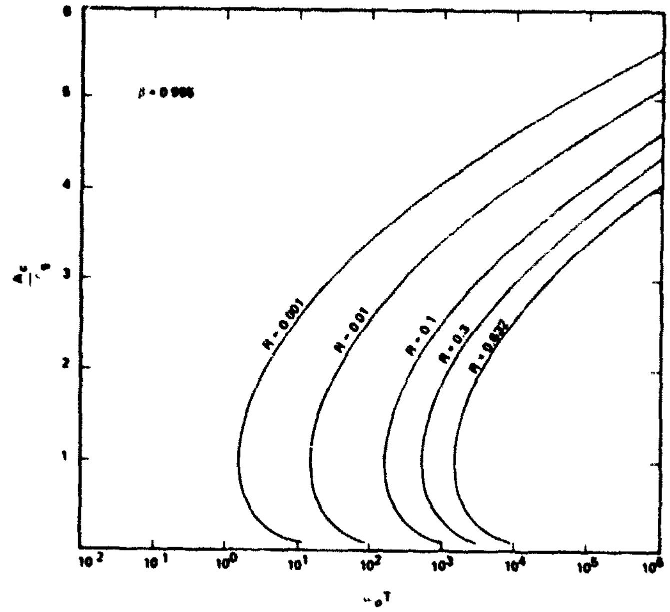

Figure 9. The quantity A_c/σ_g as a function of $\omega_o T$ and R for $\beta = 0.995$.

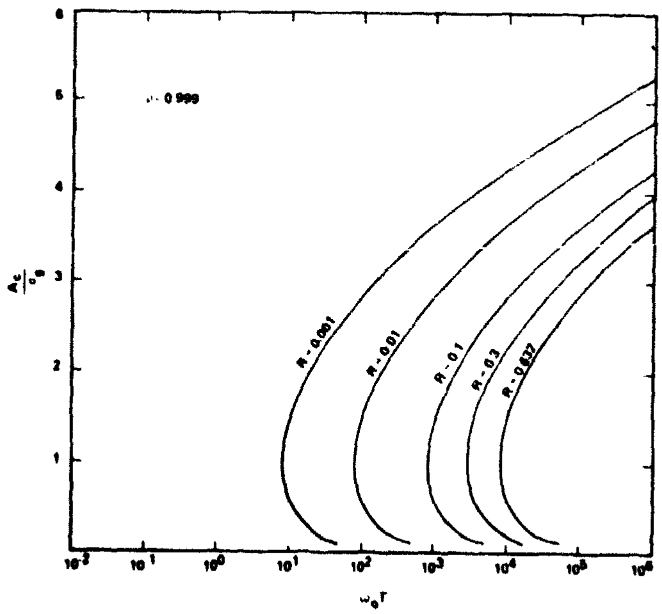

Figure 10. The quantity A_c/σ_g as a function of $\omega_o T$ and R for $\beta = 0.999$.

IV. SPACECRAFT ROTATION RATE EXCEEDANCE STATISTICS

In this section we determine the exceedance statistics of each component of the $\vec{\Omega}$ process referenced to the principal axes of the spacecraft, i.e., the (x,y,z) frame discussed in Paragraph II.C.3. Our analysis will be concerned with a single component of $\vec{\Omega}$; consequently, we will dispense with subscripts on Ω to denote components. We will use the symbol Ω to denote a component of $\vec{\Omega}$ and σ_Ω to denote the standard deviation of Ω. The developments in the subsequent sections are similar to those in the previous sections for the g process. However, the exceedance statistics of the envelope of the Ω process are not included because the available theory in the literature is valid only for random processes characterized by autospectral density functions which are symmetric about frequency ω_m on the half-interval $0 < \omega \leq \infty$; i.e., $\phi(\omega - \omega_m) = \phi(\omega + \omega_m)$. The Ω process herein does not satisfy this condition.

A. Expected Exceedance Rate of Rotation Rate

The expected number of exceedances of vehicle rotation rate per unit time which exceed level Ω is given by

$$N_\Omega = N_{\Omega,o}\, e^{-\Omega^2/2\sigma_\Omega^2} \quad . \tag{72}$$

The zero-crossing rate N_Ω is given by

$$N_{\Omega,0} = \frac{1}{2\pi}\left[\frac{\int_{-\infty}^{\infty} \omega^2 \phi_\Omega(\omega)\, d\omega}{\sigma_\Omega^2}\right]^{1/2} = \frac{\omega_o}{2\pi}\beta^{1/2} \quad , \tag{73}$$

where we have substituted equation (16) into the integral to obtain the result indicated on the right side of equation (73). The result indicated corresponds to the geometric mean frequency $(\omega_o\, \omega_1)^{1/2}$ with units of radians per second.

The ratios of the zero-crossing rates of Ω , T, and g are given by

$$\frac{N_{\Omega,0}}{N_{T,0}} = \frac{N_{\Omega,0}}{N_{g,0}} = \left[\frac{3(1-\beta)\beta}{1-\beta^3}\right]^{1/2} \quad . \tag{74}$$

$$\frac{N_{T,0}}{N_{g,0}} = 1 \quad . \tag{75}$$

Figure 11 provides a plot of $N_{\Omega,0}/N_{g,0}$ as a function of β according to equation (74) which shows that $N_{\Omega,0} < N_{g,0}$ for all relevant values of β. The reason for this result can be traced to the fact that $g(t)$ is characterized by a flat spectrum over the domain $\omega_1 < \omega \leq \omega_o$, while the spectrum of $\Omega(t)$ decreases as ω^{-2} over the same frequency domain. This means that as $|\omega|$

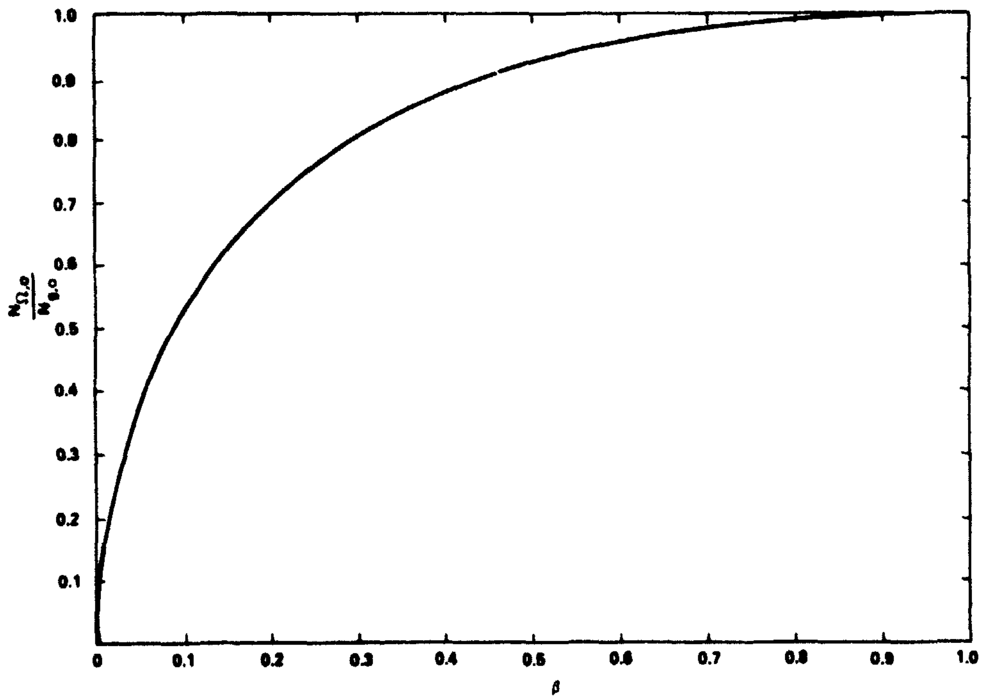

Figure 11. The ratio of the zero-crossing rate of $\Omega(t)$ to the zero-crossing rate of $g(t)$ as a function of the bandwidth parameter β.

increases from ω_1 to ω_o the Fourier components of the g process will provide increasingly larger contributions to the zero-crossing rate of $g(t)$, while the corresponding contribution to the zero-crossing rate of $\Omega(t)$ from each Fourier component of the Ω process will be the same over the bandwidth $d\omega$ for any frequency in the interval $\omega_1 < |\omega| \le \omega_o$.

Combining equations (72) and (73) yields the nondimensional exceedance rate

$$\frac{2\pi N_\Omega}{\omega_o} = \beta^{1/2} e^{-\Omega^2/2\sigma_\Omega^2} \quad . \tag{76}$$

Figure 12 contains a plot of $2\pi N_\Omega / \omega_o$ as a function of Ω/σ_Ω for $\beta = 0.01$ and 1.

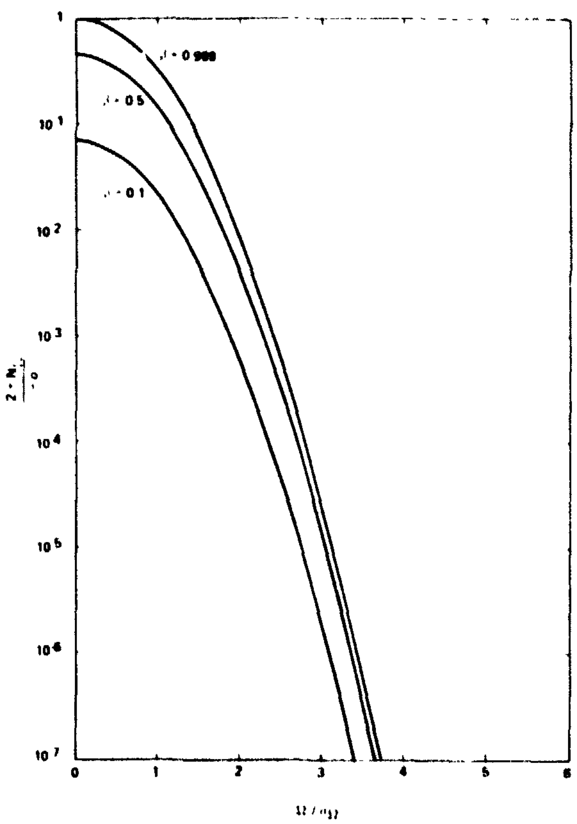

Figure 12. Nondimensional expected rate $2\pi N_\Omega / \omega_o$ of exceeding the nondimensional level $|\Omega|_c$ with positive slope for $\Omega > 0$ or negative slope for $\Omega < 0$. (The expected rate of exceeding level $|\Omega|_c/\sigma_\Omega$ with positive or negative slope is $2N_\Omega$.)

B. Risk of Rotation Rate Exceeding a Critical Value

Following the developments in Paragraph III.B, we seek to determine the risk that the $|\Omega|$ process will exceed a critical value $|\Omega|_c$ for a given orbital experiment duration time T. We hypothesize that the number of exceedances of $|\Omega|$ above level $|\Omega|_c$ from below is a Poisson process. Thus, the risk R that the $|\Omega|$ process will exceed the critical value $|\Omega|_c$ at least once during an experiment of duration time T is

$$R = 1 - e^{-2N_\Omega T} \quad . \tag{77}$$

Eliminating the expected exceedance rate N_Ω between equations (76) and (77) yields

$$\frac{|\Omega|_c}{\sigma_\Omega} = \left[-2\ln\left[-\frac{\pi}{\omega_o T \beta^{1/2}} \ln(1-R) \right] \right]^{1/2} \quad . \tag{78}$$

This formula permits the calculation of a critical rotation rate $|\Omega|_c$ as a function of risk R of the quantity $|\Omega|$ exceeding level $|\Omega|_c$ at least once during an experiment of duration time T and the Ω process spectral density parameters β and ω_o. Figures 13 and 14 contain plots of $|\Omega|/\sigma_\Omega$ as a function of $T\omega_o$ for various values of risk for $\beta = 0.01$ and 0.999, respectively.

V. CONCLUDING COMMENTS

The previous sections provide a simple stochastic model of spacecraft rotation and induced gravity. To develop the model, it was assumed that the components of the net applied torque vector are stochastically independent Gaussian processes. Validation of this model must await the results of statistical analyses of accelerometer and rate gyro data acquired from past

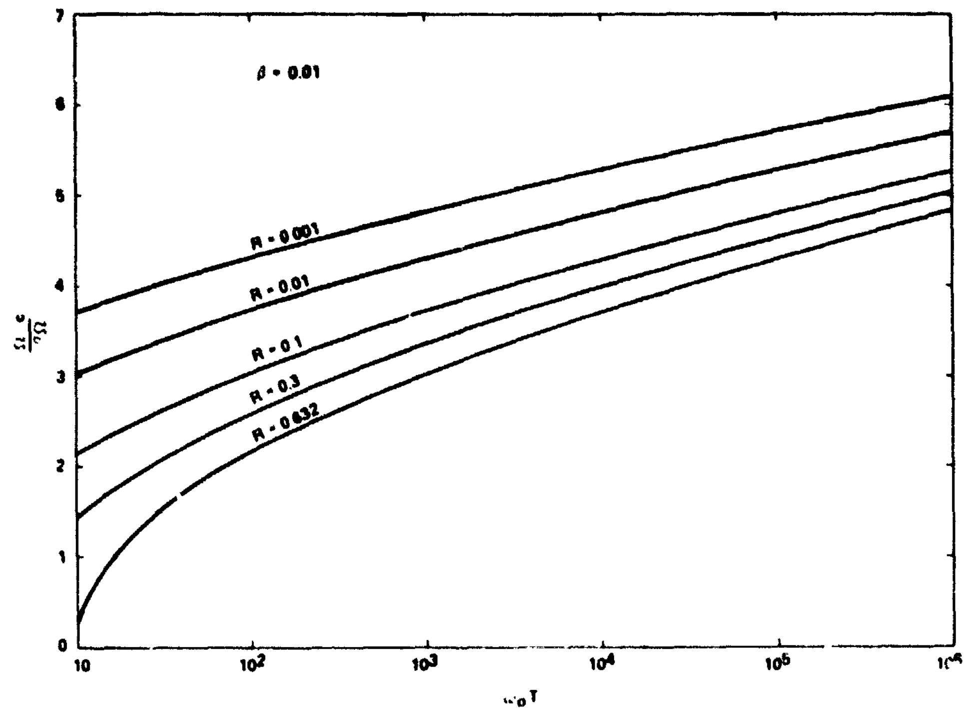

Figure 13. The quantity $|\Omega|_c/\sigma_\Omega$ as a function of $\omega_o T$ and R for $\beta = 0.01$.

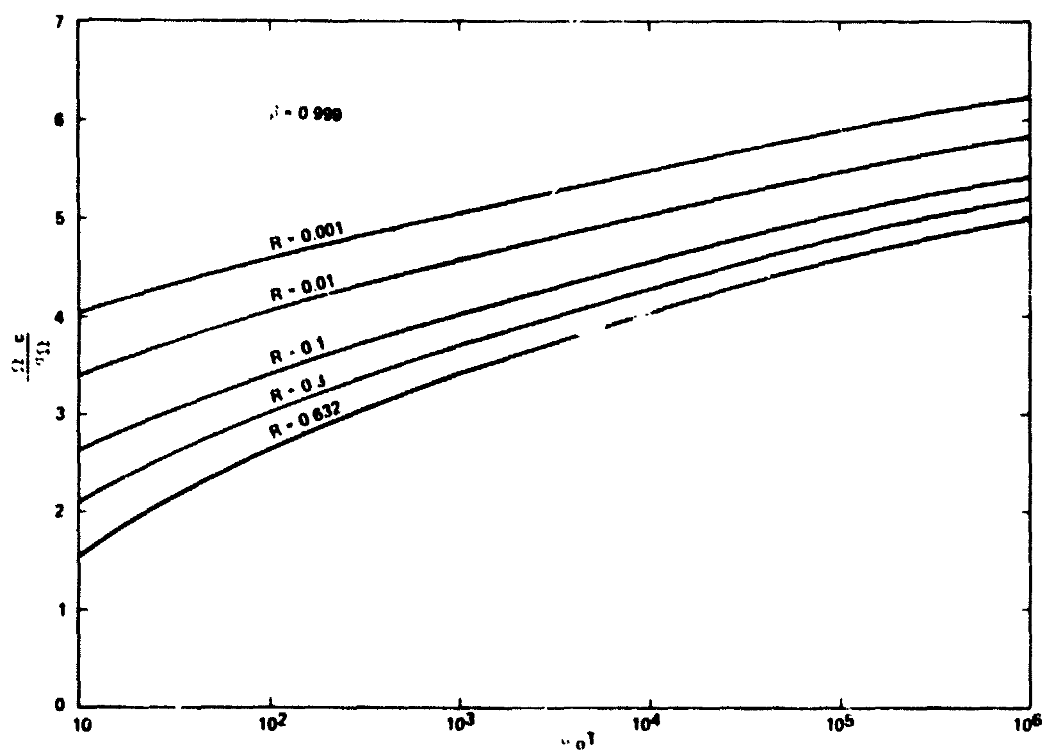

Figure 14. The quantity $|\Omega|_c/\sigma_\Omega$ as a function of $\omega_o T$ and R for $\beta = 0.999$.

spaceflight missions. The authors of this report are currently analyzing thruster rate gyro and accelerometer data acquired on the Apollo-Soyuz mission. However, in the interim time period the proposed model can be used in orbital experiment definition studies. If it is found that the components of induced gravity and vehicle rotation are non-Gaussian processes, then the calculation of risk values associated with assigned critical values of vehicle rotation and induced gravity could prove to be an extremely complex task for future spaceflight missions.

To apply the model to obtain estimates of rotation rate and induced gravity spectra and risk values associated with exceeding critical values of rotation rate and induced gravity, estimates of β, ω_o, σ_g, and σ_Ω are required. A range of values for each parameter should be used to obtain a "feel" for the effects of $\vec{g}$ and $\vec{\Omega}$ on an experiment. It should be remembered that the standard deviations of the components of the rotation and induced gravity vectors are related. In fact, the standard deviations and cross-variances of the components of $\vec{g}$ are derivable from the standard deviations of the components of $\vec{\Omega}$ via equations (18) and (28) through (34) upon specification of the vehicle principal moments of inertia and experiment location relative to the vehicle center of mass.

It should also be remembered that the model described is valid for a particular imposed torque process; i.e., the values of β, ω_o, and the standard deviations take on fixed values. However, these quantities can vary in time during a mission. To obtain exceedance statistics of g and Ω and associated risks of exceeding critical values of Ω and g for this case, the joint probability density functions $p_1(\beta, \omega_o, \sigma_\Omega)$ and $p_2(\beta, \omega_o, \sigma_g)$ for the mission are required. Considering the relationships between the standard deviations of the components $\vec{\Omega}$ and $\vec{g}$, these functions should be derivable from one another. The expected exceedance rates of Ω and g for a total mission can be obtained from the following integrals:

$$N_m(g) = \int_0^\infty \int_0^\infty \int_0^1 N(g;\beta,\omega_o,\sigma_g)\, p_1(\beta,\omega_o,\sigma_g)\, d\beta\, d\omega_o\, d\sigma_g \quad , \qquad (79)$$

$$N_m(\Omega) = \int_0^\infty \int_0^\infty \int_0^1 N(\Omega;\beta,\omega_o,\sigma_\Omega)\, p_2(\beta,\omega_o,\sigma_\Omega)\, d\beta\, d\omega_o\, d\Omega \quad . \qquad (80)$$

where N in the integrands of equations (79) and (80) are given by equations (56) and (72). The calculation of risks of exceeding critical values of g and Ω can be performed by invoking the Poisson model used in the previous sections. A similar analysis can be applied to the expected exceedance rate of the envelope of the g process. In this model for the exceedance rates of g and Ω, the torque vector process is assumed to be piecewise statistically stationary in time.

REFERENCES

1. Murrish, C. H. and Smith, G. W.: Apollo Applications Program Crew Motion Experiment Program Definition and Design Development. NASA CR-66599, 1968.

2. Conway, Bruce A. and Hendricks, T. C.: A Summary of the Skylab Crew/Vehicle Disturbances Experiment T-013. NASA TN D-8128, 1976.

3. Goldstein, H.: Classical Mechanics. Addison Wesley Publishing Company, Inc., Reading, Massachusetts, 1959.

4. Batchelor, G. K.: The Theory of Homogeneous Turbulence. Cambridge Press, London, 1960.

5. Hald, A.: Statistical Theory with Engineering Applications. John Wiley and Sons, Inc., New York, 1952.

6. Rice, S. O.: Mathematical Analysis of Random Noise. Bell System Technical Journal, vol. 24, 1944, pp. 282-332.

7. Mathematical Analysis of Random Noise. Bell System Technical Journal, vol. 24, 1945, pp. 46-156.

8. Lin, Y. K.: Probabilistic Theory of Structural Dynamics. McGraw-Hill Book Company, New York, 1967.

APPROVAL

SIMPLIFIED MODEL OF STATISTICALLY STATIONARY SPACECRAFT ROTATION AND ASSOCIATED INDUCED GRAVITY ENVIRONMENTS

By George H. Fichtl and Robert L. Holland

The information in this report has been reviewed for security classification. Review of any information concerning Department of Defense or nuclear energy activities or programs has been made by the MSFC Security Classification Officer. This report, in its entirety, has been determined to be unclassified.

William W. Vaughan

WILLIAM W. VAUGHAN
Chief, Atmospheric Sciences Division

Charles A. Lundquist

CHARLES A. LUNDQUIST
Director, Space Sciences Laboratory